JOURNAL OF BACTERIOLOGY, Feb. 2009, p. 909–921 Vol. 191, No. 3
0021-9193/09/$08.00+0 doi:10.1128/JB.01419-08

Evolution of Penicillin-Binding Protein 2 Concentration and Cell Shape during a Long-Term Experiment with *Escherichia coli*▽

Nadège Philippe,[1,2]† Ludovic Pelosi,[1,2]†‡ Richard E. Lenski,[3] and Dominique Schneider[1,2]*

Laboratoire Adaptation et Pathogénie des Micro-organismes, Université Joseph Fourier Grenoble 1, BP 170, F-38042 Grenoble cedex 9, France[1]; CNRS UMR 5163, F-38042 Grenoble Cedex 9, France[2]; and Department of Microbiology and Molecular Genetics, Michigan State University, East Lansing, Michigan 48824[3]

Received 9 October 2008/Accepted 17 November 2008

Peptidoglycan is the major component of the bacterial cell wall and is involved in osmotic protection and in determining cell shape. Cell shape potentially influences many processes, including nutrient uptake as well as cell survival and growth. Peptidoglycan is a dynamic structure that changes during the growth cycle. Penicillin-binding proteins (PBPs) catalyze the final stages of peptidoglycan synthesis. Although PBPs are biochemically and physiologically well characterized, their broader effects, especially their effects on organismal fitness, are not well understood. In a long-term experiment, 12 populations of *Escherichia coli* having a common ancestor were allowed to evolve for more than 40,000 generations in a defined environment. We previously identified mutations in the *pbpA* operon in one-half of these populations; this operon encodes PBP2 and RodA proteins that are involved in cell wall elongation. In this study, we characterized the effects of two of these mutations on competitive fitness and other phenotypes. By constructing and performing competition experiments with strains that are isogenic except for the *pbpA* alleles, we showed that both mutations that evolved were beneficial in the environment used for the long-term experiment and that these mutations caused parallel phenotypic changes. In particular, they reduced the cellular concentration of PBP2, thereby generating spherical cells with an increased volume. In contrast to their fitness-enhancing effect in the environment where they evolved, both mutations decreased cellular resistance to osmotic stress. Moreover, one mutation reduced fitness during prolonged stationary phase. Therefore, alteration of the PBP2 concentration contributed to physiological trade-offs and ecological specialization during experimental evolution.

Bacteria in nature must survive multiple stresses and repeated shifts between feast and famine conditions. When *Escherichia coli* experiences nutritional deprivation, its growth rate decreases sharply and the cells become more spherical and resistant to various other environmental stresses (27). Many of the morphological and physiological changes that occur during entry into "stationary" phase are associated with the cell envelope, especially the cell wall.

Peptidoglycan is the major component of the bacterial cell wall, and it affects osmotic stability and cell shape (78). Many of the final steps of peptidoglycan synthesis are catalyzed in the periplasm by the penicillin-binding proteins (PBPs) (40, 82). These enzymes are named for their binding to β-lactam antibiotics that inhibit cell wall biosynthesis. Twelve PBPs have been identified so far in *E. coli*, and they are classified as high-molecular-weight (HMW) and low-molecular-weight (LMW) PBPs. The HMW PBPs assemble both the glycan chain and the peptide cross-links of peptidoglycan and are further divided into class A PBPs (PBP1a, PBP1b, and PBP1c), which are bifunctional enzymes that perform both transglycosylation and transpeptidation functions, and class B PBPs (PBP2 and PBP3), which are monofunctional transpeptidases (24). The LMW PBPs (PBP4, PBP5, PBP6, PBP7, DacD, AmpC, and AmpH) are monofunctional, and they modify peptidoglycan by either carboxypeptidase or endopeptidase activities (53).

Numerous studies have investigated the physiological roles of PBPs by mutating either the PBP-encoding genes or by inactivating the corresponding proteins using specific β-lactam antibiotics. Although the class A HMW PBPs are peptidoglycan synthases, their physiological role is still unclear. Multiple *Bacillus subtilis* mutants are viable, although they have increased average cell lengths and reduced cell diameters (41, 53), whereas in *E. coli* the absence of two class A PBPs caused cell lysis (83). The two *E. coli* class B HMW PBPs, PBP2 and PBP3, are the only HMW PBPs that are essential for cell elongation and division, respectively. Loss of PBP2 results in cells that are spherical instead of rod shaped; PBP2 mutants are unable to grow and divide in rich media (18) unless compensatory mutations are present (75, 76). By contrast, PBP3 is involved in peptidoglycan synthesis during septation, and the absence of PBP3 causes cell filamentation (10, 65). The LMW PBPs have been shown to be involved in the control of cell shape, and severe shape abnormalities have been detected in mutants defective for several of these PBPs (44, 45, 53).

It is often necessary to inactivate several PBP-encoding genes to observe a clear phenotypic effect, which raises interesting questions about the biological significance of each individual PBP, such as whether single mutations may have more

* Corresponding author. Mailing address: Laboratoire Adaptation et Pathogénie des Microorganismes, Institut Jean Roget, CNRS UMR5163, Université Joseph Fourier, Campus Santé, Domaine de la Merci, BP170, 38042 Grenoble Cedex 9, France. Phone: (33) 4 76 63 74 90. Fax: (33) 4 76 63 74 97. E-mail: dominique.schneider@ujf-grenoble.fr.

† N.P. and L.P. contributed equally to this study.

‡ Present address: Laboratoire de Biochimie et Biophysique des Systèmes Intégrés (BBSI), Institut de Recherches en Technologies et Sciences du Vivant (iRTSV), UMR 5092 CNRS-CEA-Université Joseph Fourier (UJF), CEA-Grenoble, 17 Avenue des Martyrs, 38054 Grenoble Cedex 9, France.

▽ Published ahead of print on 1 December 2008.

subtle effects on phenotypes such as competitive fitness. An *E. coli* mutant lacking as many as 8 of the 12 PBPs (PBP4, PBP5, PBP6, PBP7, AmpC, AmpH, DacD, and either PBP1a or PBP1b) is viable (17). Even shape aberrations may become noticeable only when multiple LMW PBP-encoding genes are inactivated (53). In a recent study, the physiological relevance of 10 PBPs for survival during prolonged starvation was investigated (51), and in this environment PBP1b was shown to be required for long-term persistence. The same mutant was also more sensitive to osmotic stress. However, nine other PBPs (PBP1a, PBP1c, PBP4, PBP5, PBP6, PBP7, AmpC, AmpH, and DacD) were apparently dispensable for survival during starvation. Two other PBPs, PBP2 and PBP3, could not be evaluated because inactivation of the corresponding genes resulted in severe defects. In that study, all the mutations were deliberately constructed and subsequently tested to determine their effects on fitness, in contrast to mutations that may arise spontaneously and be substituted by natural selection. Here, we describe functional analyses of mutations within the operon containing the *pbpA* gene (referred to below as the *pbpA* operon), encoding the PBP2 and RodA proteins, that evolved in *E. coli* during a long-term experiment.

Twelve populations of *E. coli* were founded in 1988 using a common ancestor and have been propagated by daily serial transfer, after 1:100 dilution, in a defined glucose-limited medium for more than 40,000 generations (33, 36, 38). These populations experience a daily cycle of regrowth in fresh medium followed by a transition into stationary phase, during which the cells starve until the next transfer into fresh medium. The environment therefore imposes repeated bouts of feast and famine. A "frozen fossil record" is available because samples of each population have been conserved at regular intervals throughout the experiment. Substantial adaptive evolution has occurred in all of the replicate populations, as they exhibited similar gains in competitive fitness (on average, about 70%) after 20,000 generations (13). (In other words, an evolved population grew about 70% faster than its ancestor while the two populations competed with one another using the same serial transfer regimen that was used in the evolution experiment.) Several other phenotypic traits also evolved in parallel in most or all of the populations. The most visually apparent of these traits is a substantial increase in the average cell size in all 12 populations (35). Other parallel phenotypic changes include faster exponential growth and a shorter lag phase (74), reduced catabolic breadth (13), and increased DNA superhelicity (14). Also, global transcriptional and proteomic profiles were obtained for two populations, and significant parallel changes were observed in the expression of dozens of genes (11, 50).

To date, three types of genetic and molecular analyses have been performed with the evolved lines, which has allowed discovery of mutations in about 10 genes (52). First, some mutations were found in candidate genes known to affect certain phenotypes that changed conspicuously in some or all of the evolved populations. All 12 lines lost the capacity to grow on ribose, and deletions in the *rbs* operon were found in all of them (12). Also, three lines became mutators by 10,000 generations, and the underlying mutations were found in the *mutL* and *mutS* genes (62, 64). Second, analyses of global gene expression profiles and regulatory networks for two focal populations allowed us to discover mutations in the *spoT*, *topA*, and *fis* genes involved in the stringent response and DNA topology regulatory networks, respectively (11, 14, 50), and in the *malT* gene involved in maltose consumption (50). Third, insertion sequence (IS) elements were used as genomic markers to find mutations in the same two focal populations (48, 61). A total of four IS*150* insertions were found; these insertions were located within the *pykF* gene encoding pyruvate kinase I (8), within the *nadR* gene encoding the repressor of the NAD biosynthetic genes (26), within the *hokB* locus homologous to plasmid addiction modules (49), and 11 bp upstream of the putative promoter of the *pbpA* operon encoding PBP2 and RodA, which are involved in cell wall biosynthesis and determination of the cell shape (5).

The gene expression and IS element studies were performed with only two populations, so the relevant loci were subsequently sequenced and analyzed in all 12 populations (11, 50, 79; E. Crozat, C. L. Winkworth, J. Gaffé, P. F. Hallin, M. A. Riley, R. E. Lenski, and D. Schneider, unpublished data). These analyses uncovered numerous examples of genetic parallelism, in which the same loci also harbored mutations in many or all of the other populations. Of particular relevance to the present study, mutations were found in the *pbpA* operon in one-half of the populations (Fig. 1). This parallelism is in striking contrast to data obtained by a sequencing analysis of 36 genes chosen at random, in which almost no mutations were detected and no gene was affected in more than one population (34). Several statistical tests provided strong support for

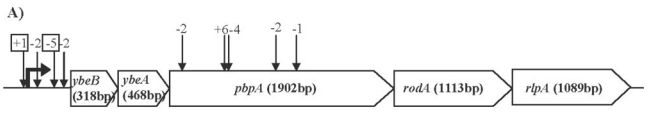

B)

Population	Position	Mutation	Amino acid change
Ara-1	1411	A→T	Ile → Phe
Ara-2 (M)	-873	T→C	Non coding
Ara-2 (M)	-742	C→T	Non coding
Ara-2 (M)	141	T→G	Phe → Leu
Ara-2 (M)	1280	G→A	Gly → Asp
Ara-4 (M)	761	T→C	Leu → Pro
Ara-5	-800	A→T	Non coding
Ara+1	-904	::IS*150*	Non coding
Ara+6 (M)	748	A→C	Ile → Leu

FIG. 1. Mutations identified in the *pbpA* operon in evolving *E. coli* populations (adapted from references 61 and 79). (A) Organization of the operon and location of mutations in populations Ara-1, Ara-2, Ara-4, Ara-5, Ara+1, and Ara+6. The operon includes five genes; *ybeA* and *ybeB* encode proteins with unknown functions, *pbpA* encodes PBP2, *rodA* encodes the RodA protein, and *rlpA* encodes a rare lipoprotein. Both PBP2 and RodA are involved in cell wall elongation and cell morphogenesis. The size of each coding region is indicated. The locations of evolved mutations are indicated by arrows, and the populations in which they occurred are indicated above the arrows. The two evolved *pbpA* alleles studied in this work are enclosed in boxes (Ara-5 and Ara+1). The bent arrow upstream of *ybeB* indicates the operon's putative promoter (2). (B) Characteristics of the evolved mutations, including the populations in which they arose, their positions relative to the first nucleotide of the translation initiation codon of *pbpA*, their molecular nature, and their consequences for the amino acid sequence. Several populations, indicated by (M), evolved mutator phenotypes and had substantially elevated mutation rates. Population Ara+1 acquired an IS*150* insertion (::IS*150*). Mutations in the regulatory region are indicated by "Non coding."

the conclusion that the parallel mutations conferred selective advantages to the bacteria under the conditions that prevailed during the evolution experiment (79). This conclusion was confirmed for several loci by performing direct competition between isogenic strains that differ only by mutations in the affected genes. To date, however, no competition experiments have been performed to test the fitness effects of the evolved *pbpA* alleles, nor have any phenotypic traits been shown to be caused by the mutations found in the *pbpA* operon.

Therefore, in this study, we sought to characterize the effects on competitive fitness and other phenotypic traits of two independently evolved mutations in the *pbpA* operon. We demonstrate here that both mutations were beneficial under the conditions used in the long-term evolution experiment. We also show that both mutations led to other parallel phenotypic changes, including contributing to the increased cell size observed in the evolving populations, as well as pleiotropic effects shown by trade-offs in performance in other environments.

MATERIALS AND METHODS

Bacterial strains and plasmids. A derivative of *E. coli* B (31, 60) was used as the common ancestor to initiate 12 populations that have been serially propagated in the same glucose-limited minimal medium for more than 40,000 generations (9, 13, 33, 36, 38). Six of the populations, designated Ara-1 to Ara-6, were initiated from strain REL606, which is unable to use arabinose as a carbon source (Ara$^-$), whereas the other six populations, designated Ara+1 to Ara+6, were initiated from an Ara$^+$ mutant, REL607, of the same strain. Ara$^-$ and Ara$^+$ cells produce red and white colonies, respectively, on tetrazolium-arabinose indicator plates (38). During competition experiments, the Ara phenotype provides a marker that has been demonstrated to be selectively neutral in the glucose-limited environment (36, 38). At 500-generation intervals throughout the evolution experiment, samples were obtained from each population and frozen as glycerol suspensions at −80°C.

A total of nine mutations in the *pbpA* operon were found in six populations after 20,000 generations (79). Population Ara-2 had four mutations, while populations Ara-1, Ara-4, Ara-5, Ara+1, and Ara+6 had one each (Fig. 1). Populations Ara-2, Ara-4, and Ara+6 had become mutators by 20,000 generations, whereas the three other populations with mutations in the *pbpA* operon had not become mutators (13, 64). To avoid possible complications arising from secondary mutations in mutator lineages, we focused on the evolved *pbpA* alleles that were substituted in nonmutator populations Ara-1, Ara-5, and Ara+1. Despite numerous attempts, we were unable to move the Ara-1 evolved allele into the ancestral chromosome; we do not understand why this difficulty occurred. In any case, we focused on the evolved alleles $pbpA_{-5}$ and $pbpA_{+1}$ that were substituted in populations Ara-5 and Ara+1, respectively.

From the "frozen fossil record" kept throughout the long-term evolution experiment, we used heterogeneous samples and individual evolved clones isolated at different generations from the same two populations, Ara-5 and Ara+1. These samples and clones are described in Table 1, as are strains derived from them by construction of otherwise isogenic chromosomes with different alleles of the *pbpA* operon (see below).

For cloning experiments, we used *E. coli* JM109 (80) and standard procedures (57) or TOP10 (Invitrogen) according to the supplier's recommendations. We used plasmids pCRII-Topo (Invitrogen) and pKO3 (39) for cloning experiments and allelic replacement, respectively. Transcriptional fusions with *lacZ* as a reporter gene were constructed using plasmid pRS551 (63).

Growth conditions and media. Strains were grown either in rich LB medium (57) or in Davis minimal medium supplemented with one of two glucose concentrations, 25 μg/ml (DM25) (the concentration used in the evolution experiment) (38) or 250 μg/ml (DM250) (to obtain denser cell cultures). Infections with phage λ were performed after bacteria were grown in TBMM medium (10 g/liter tryptone, 5 g/liter NaCl, 0.2% maltose, 10 mM $MgSO_4$, 1 μg/ml thiamine). Chloramphenicol (30 μg/ml), ampicillin (100 μg/ml), kanamycin (50 μg/ml), and nalidixic acid (20 μg/ml) were added as needed.

Agar (Difco) was added at a concentration of 12 g/liter to LB medium to obtain rich medium for plating cells. Selection for sucrose-resistant clones during allelic exchange experiments was performed by plating cells onto sucrose plates in which 5% sucrose but no NaCl was added to the LB plating medium. To distinguish Ara$^-$ clones from Ara$^+$ clones, cells were spread onto tetrazolium-arabinose indicator plates (10 g/liter tryptone, 1 g/liter yeast extract, 5 g/liter NaCl, 0.05% antifoam agent, 1% arabinose, 0.005% tetrazolium, 12 g/liter agar). All experiments and procedures were performed at 37°C unless otherwise noted.

TABLE 1. Bacterial strains used in this study

Strain	Description	Reference(s)
REL606	*E. coli* B Bc251 T6^r Str^r rm_{III} Ara$^-$ ($pbpA_{anc}$)[a]	31, 60
REL607	Ara$^+$ revertant of REL606 ($pbpA_{anc}$)[a]	38
REL768	500-generation mixed sample of population Ara+1	38
REL958	1,000-generation mixed sample of population Ara+1	38
REL1062	1,500-generation mixed sample of population Ara+1	38
REL1158	2,000-generation mixed sample of population Ara+1	38
REL1158A	2,000-generation clone from population Ara+1 ($pbpA_{anc}$)[a]	38
REL1158C	2,000-generation clone from population Ara+1 ($pbpA_{+1}$)[a]	38
REL766	500-generation mixed sample of population Ara-5	38
REL968	1,000-generation mixed sample of population Ara-5	38
REL1072	1,500-generation mixed sample of population Ara-5	38
REL1168	2,000-generation mixed sample of population Ara-5	38
REL968-8	1,000-generation clone from population Ara-5 ($pbpA_{-5}$)[a]	This study
DVS53	REL1158C $pbpA_{anc}$[a]	This study
DVS79	REL968-8 $pbpA_{anc}$	This study
LUD5	REL606 $pbpA_{-5}$[a]	This study
LUD6	LUD5 with $pbpA_{-5}$ restored to $pbpA_{anc}$[a]	This study

[a] For individual clones, $pbpA_{anc}$ indicates the ancestral allele, while $pbpA_{+1}$ and $pbpA_{-5}$ indicate the evolved alleles from populations Ara+1 and Ara-5, respectively.

Strain construction. We performed two sets of allelic replacement procedures. First, the evolved *pbpA* operon from population Ara-5 was moved into the Ara$^-$ ancestral background. Second, the evolved *pbpA* operons from populations Ara+1 and Ara-5 were replaced by the ancestral *pbpA* allele (from REL606). The Ara+1 evolved allele was not moved into the ancestral background because this allele has an IS*150* element that is inserted upstream of the *pbpA* operon and our efforts to move this allele invariably led to unintended recombination with other copies of the IS*150* elements present in the ancestral strain (48). All gene replacement experiments were performed by using suicide plasmid pKO3, which has a temperature-sensitive origin of replication (39), as described in detail elsewhere (14).

Briefly, DNA fragments containing either the evolved $pbpA_{-5}$ allele or the ancestral *pbpA* allele ($pbpA_{anc}$) were PCR amplified using primers ODS305 (5′ GACAATGCGGTTTTTGCCTG 3′) and ODS306 (5′ GTGGAACGCTTTAT CGCAAG 3′), while the ancestral counterpart of the $pbpA_{+1}$ allele was obtained with primers G167 (5′ ACGACGCAGGTACTCGGTA 3′) and G168 (5′ CTC ATGCAAGAAGATGCCG 3′). The three PCR products were cloned into the suicide plasmid pKO3. The plasmids carrying ancestral alleles were electrotransformed into evolved clones isolated from the Ara+1 and Ara-5 populations, while the plasmid bearing the evolved $pbpA_{-5}$ allele was introduced into the ancestral strain. In each case, integration of the nonreplicative plasmid into the chromosomal *pbpA* operon was selected by plating transformed cells on LB agar containing chloramphenicol and incubating the preparation at the restrictive temperature. Chloramphenicol-resistant clones were then streaked on sucrose agar to select for sucrose-resistant cells that had lost the plasmid, because pKO3 carries the *sacB* gene, whose product makes the host susceptible to killing by sucrose. The plasmid-free cells were then screened for the presence of the ancestral or evolved *pbpA* allele, either by measuring the length of the PCR

product containing the *pbpA* operon for population Ara+1 or by using a PCR-restriction fragment length polymorphism approach with restriction enzyme GsuI (Fermentas) to distinguish between ancestral and evolved alleles from population Ara-5. To control for possible secondary mutations that might have occurred during strain construction, we performed reciprocal "deconstruction experiments," in which each introduced allele was removed and replaced with the original allele (11). The resulting strains were used as controls for assessing the reversion of all relevant phenotypes (fitness, PBP levels, and cell size), and complete reversion indicated that there were no secondary mutations that would otherwise complicate the analyses.

Measurement of cell morphology and cell volume. Each strain was grown in DM250 to mid-exponential phase (optical density at 600 nm [OD_{600}], 0.2), and cells were observed using a Zeiss Axioplan 2 microscope. In some cases, as noted below, 4 μg/ml of amdinocillin was added to the cultures after 1 h of incubation; cells were then incubated for an additional 5 h and observed.

Average cell volumes were estimated at stationary phase following two daily cycles of growth in DM25 under the same conditions that were used in the long-term evolution experiment and then 1:100 dilution in isotone solution (Beckman). Cell volumes were analyzed using a Coulter Multisizer 3 counter (Beckman). The mean cell volume was estimated by using six replicate cultures and a total of about 300,000 cells for each strain analyzed.

Construction of *pbpA-lacZ* transcriptional fusions. The ancestral and evolved promoter regions of the *pbpA* operon were PCR amplified using primers ODS298 (5′ GGGGTCGAGAATTCATGACTTTTC 3′) and ODS299 (5′ GG CTGGACGGATCCGTACAGATGA 3′) and cloned into pRS551 (63), which generated transcriptional fusions with *lacZ* as a reporter. These fusions were then crossed in vivo into the λRS45 bacteriophage derivative, which was followed by lysogenization of the ancestral strain REL606 at the chromosomal *att*(λ) site, as described previously (63). A PCR assay was performed to confirm that only a single prophage was integrated (54).

The same protocol was not used for the fusion with the $pbpA_{+1}$ promoter region, however, because this evolved allele has an IS*150* insertion (61) that might lead to difficulties in introducing a single copy of the fusion into *att*(λ). Therefore, the activity of the evolved $pbpA_{+1}$ promoter was instead analyzed using a plasmid fusion. Specifically, the plasmid carrying the P$pbpA_{+1}$::*lacZ* fusion was introduced into the ancestral strain REL606, and its β-galactosidase activity was compared to the activities obtained with both pRS551, which lacks any insert, and the P$pbpA_{anc}$::*lacZ* fusion.

The β-galactosidase activities were assayed by using *o*-nitrophenyl-β-D-galactopyranoside as a substrate and were expressed in μmol *o*-nitrophenol min^{-1} mg^{-1} cellular protein (42). All the activity values reported below are the averages of three independent assays.

Membrane preparations. Each strain was grown for 16 h at 37°C in 500 ml DM250. Cells were harvested by centrifugation (4,000 × *g*, 10 min, 4°C), washed with 50 ml of 70 mM Tris-HCl (pH 7.4), and resuspended in 20 ml of the same buffer. Cells were disrupted using a French press (ThermoSpectronic) at 1,000 lb/in^2. Cell fragments, nucleic acids, and unbroken cells were concentrated by centrifugation (4,000 × *g*, 10 min, 4°C) and discarded. Membranes were then sedimented by ultracentrifugation (50,000 × *g*, 1 h, 4°C). The resulting pellet was resuspended in 250 to 500 μl of 70 mM Tris-HCl (pH 7.4) containing 10% (vol/vol) glycerol and stored at −80°C. The protein concentration was determined by performing a Bradford assay (Bio-Rad) with bovine serum albumin as the standard.

Detection of PBP2 by Western blotting. Forty micrograms of membrane proteins was diluted in 70 mM Tris-HCl (pH 7.4) and mixed with 5 μM fluorescein-conjugated ampicillin (a gift from Galleni Moreno), which binds specifically to PBPs (final volume, 20 μl). The samples were incubated for 30 min to 1 h at 30°C and then subjected to 8% sodium dodecyl sulfate-polyacrylamide gel electrophoresis. Immunoblot analyses of proteins that were electrotransferred (Bio-Rad) onto polyvinylidene difluoride membranes (Amersham Pharmacia) were performed with horseradish peroxidase-conjugated antifluorescein antibodies (Roche). The blots were developed using the enhanced chemiluminescence method by following the supplier's recommendations (Amersham Pharmacia).

To specifically identify PBP2 on the immunoblots, an amdinocillin competition assay was performed. Prior to addition of ampicillin, one half of the membrane protein samples were treated for 30 min to 1 h at 30°C with 4 μg/ml amdinocillin. This antibiotic specifically binds and inactivates PBP2 (66), thereby competing with fluorescein-conjugated ampicillin for binding to PBP2 and inhibiting its fluorescent labeling. Water was added to the other half of the samples as a control. The resulting comparison between amdinocillin-treated and untreated samples allowed specific identification and quantification of PBP2.

Sensitivity to osmotic stress. Four replicate cultures of each strain were diluted 1:100 in LB medium containing 0, 0.1, 0.2, 0.4, or 0.6 M NaCl by using overnight cultures in LB medium. After 12 h of incubation at 37°C, each culture was sampled and serial dilutions were plated onto LB agar. The plates were then incubated for 24 h at 37°C. The effect of osmotic stress on net population growth, which reflected differences in both growth and survival, was estimated from the ratio of the numbers of colonies for cells grown in the presence and in the absence of NaCl.

Fitness assays. Pairwise competition experiments were performed to estimate the fitness effects of the evolved and ancestral *pbpA* alleles. In all cases, the competing strains also differed by the neutral Ara marker, which allowed them to be distinguished by colony color on tetrazolium-arabinose plates. To ascertain the effect of the evolved $pbpA_{-5}$ allele, the Ara^+ variant of the ancestral strain, REL607 ($pbpA_{anc}$), was used in competition experiments with the following three Ara^- strains: the ancestor REL606 strain ($pbpA_{anc}$); LUD5 (REL606 $pbpA_{-5}$), in which the evolved $pbpA_{-5}$ allele was moved to the ancestral chromosome; and LUD6 (LUD5 $pbpA_{anc}$), in which the ancestral allele was restored. To measure the effect of the $pbpA_{+1}$ allele, the Ara^- ancestor, REL606 ($pbpA_{anc}$), was used in competition experiments with the following three Ara^+ strains: the ancestral REL607 strain ($pbpA_{anc}$); REL1158C, a clone isolated at generation 2000 that carries the evolved $pbpA_{+1}$ allele; and DVS53 (REL1158C $pbpA_{anc}$), in which the ancestral allele was moved into the evolved clone. The competition experiments were performed for 1 or 6 days (with 1:100 daily transfers), and the longer assays allowed detection of smaller fitness effects. Each pairwise competition experiment was replicated either five or six times. All competition experiments were performed using the same medium and other conditions that were used during the evolution experiment; hence, the assays encompassed the same phases of population growth, including lag, exponential, and stationary phases (38, 74). Prior to each assay, the competitors were separately acclimated to the same regimen and then transferred together from stationary-phase cultures into fresh medium (each diluted 1:200; thus, 1:100 combined dilution). Samples were taken immediately after mixing on day 0 and then again after 1 or 6 days of competition in order to measure the abundance of each competitor. From the initial and final densities and the known dilution factor, we calculated the realized (net) population growth of each competitor. Fitness was then calculated by determining the ratio of the realized growth rates of the two strains during the direct competition. We performed *t* tests to evaluate whether the measured relative fitness values differed significantly from the null hypothetical value, which was 1.

We also tested for differences in competitiveness and survival between the ancestral and evolved $pbpA_{-5}$ alleles during a prolonged stationary phase in LB medium using the same strains (REL607, REL606, LUD5, and LUD6) that were used in the standard competition assays described above. Also, survival was measured for each strain using a monoculture. Long-term survival was measured by inoculating 5-ml LB medium cultures (1:1,000 dilution) using overnight cultures that had been initiated from frozen glycerol stocks of each of the four strains, as previously described (84). Briefly, cultures were grown in triplicate with agitation at 37°C, and viable cell counts were determined daily by plating serial dilutions of the cultures onto LB agar. For these stationary-phase competition experiments, the competitors were also marked with a mutation conferring resistance to nalidixic acid. Each pairwise competition experiment was performed twice, with the marker present in turn in each of the competitors to control for any marker-associated effect; each reciprocal pair was then replicated three times. The competing strains were grown separately for 24 h in LB medium prior to mixing, which allowed them to enter and acclimate to stationary phase. Cultures were then mixed 1:1,000, and the densities of the two competitors were monitored for 15 days by serial dilution and plating on LB agar both with and without nalidixic acid.

Evolutionary dynamics of *pbpA* allelic substitutions. The approximate time of origin and subsequent dynamics of the *pbpA* mutations substituted in populations Ara+1 and Ara-5 were analyzed by PCR using clones isolated from samples frozen at different time points during the long-term experiment. For population Ara+1, numerous clones obtained after 500, 1,000, 1,500, and 2,000 generations were subjected to PCR using primers ODS298 and ODS299, and the ancestral and evolved alleles were distinguished by the sizes of the PCR products. For population Ara-5, clones obtained after 500, 1,000, and 2,000 generations were subjected to PCR using the same primers, followed by restriction of the PCR products with GsuI (Euromedex) to classify the *pbpA* allele as either ancestral or evolved.

RESULTS

Evolved *pbpA* alleles reduce the expression of PBP2. Both evolved alleles studied here have mutations in the promoter region of the *pbpA* operon (Fig. 1), and so we analyzed their

TABLE 2. Effects of evolved *pbpA* alleles on transcription

Promoter fused to *lacZ*[a]	β-Galactosidase activity[b]	
	Exponential phase	Stationary phase
P$pbpA_{anc}$[c]	100	100
P$pbpA_{-5}$[c]	7.35 ± 0.67	12.87 ± 0.58
P$pbpA_{anc}$[d]	100	100
P$pbpA_{+1}$[d]	45 ± 4	51 ± 5

[a] The promoters studied were the ancestral promoter, P$pbpA_{anc}$, and the evolved promoters P$pbpA_{-5}$ and P$pbpA_{+1}$ from populations Ara-5 and Ara+1, respectively.

[b] The values are the averages ± standard deviations of three separate cultures; the values for the ancestral promoter were arbitrarily defined as 100. Cultures were grown in DM250 at 37°C, and samples were withdrawn at exponential phase (OD_{600}, 0.2) and at stationary phase after 24 h. The β-galactosidase specific activities are expressed in μmol *o*-nitrophenol min^{-1} mg^{-1} cellular protein (42).

[c] Transcriptional fusions P$pbpA_{anc}$::*lacZ* and P$pbpA_{-5}$::*lacZ* were introduced as single copies into the chromosome of the ancestral strain, REL606, at the bacteriophage λ attachment site.

[d] The P$pbpA_{anc}$::*lacZ* and P$pbpA_{+1}$::*lacZ* fusions were constructed on the pRS551 plasmid and then moved into REL606. The residual activity of pRS551 without any insert was deducted from the β-galactosidase activities measured for P$pbpA_{anc}$ and P$pbpA_{+1}$.

effects on the transcription of this operon. The strains carrying *pbpA*::*lacZ* transcriptional fusions were grown in DM250, and samples were taken at mid-log phase (OD_{600}, 0.2) and again during stationary phase (total incubation time, 24 h). The transcriptional levels of each *pbpA* construct were then analyzed by monitoring β-galactosidase activities.

Both evolved mutations in the *pbpA* promoter region caused substantial reductions in the transcription of the operon (Table 2). The evolved $pbpA^{-5}$ allele led to 14- and 8-fold reductions during the exponential and stationary phases, respectively, while the evolved $pbpA_{+1}$ allele caused a 2-fold decline in each phase. However, the apparent difference in the relative effects of the evolved promoters is not necessarily meaningful, because the corresponding fusions were chromosomal for $pbpA_{-5}$ and plasmidic for $pbpA_{+1}$, for reasons explained in Materials and Methods.

To confirm and extend these results, we assessed the amounts of PBP2 in the ancestor, various evolved clones, and isogenic constructs that differed only in their *pbpA* alleles. Cell membranes were prepared from these strains as described in Materials and Methods, and PBPs were detected after labeling with fluorescein-conjugated ampicillin and using horseradish peroxidase-conjugated antifluorescein antibodies. Specific identification of PBP2 was performed by using competitive binding of amdinocillin, which was added prior to the fluorescein-conjugated ampicillin labeling step. Therefore, the PBP2 band should have specifically disappeared after the competitive treatment, allowing identification of PBP2 in the untreated samples (Fig. 2).

In the ancestral strain REL606, one unique band specifically disappeared after amdinocillin competition, and therefore this band corresponded to PBP2 (Fig. 2). In the untreated samples, the amount of PBP2 depended on the *pbpA* allele (Fig. 2). In particular, the levels of PBP2 observed in the evolved clones from populations Ara-5 and Ara+1 carrying the evolved *pbpA* alleles (REL968-8 and REL1158C) and after $pbpA_{-5}$ was moved into the ancestor (LUD5) were lower than the levels in the ancestral strain REL606. Moreover, replacement of $pbpA_{+1}$ by $pbpA_{anc}$ in the evolved clone REL1158C restored the ancestral level of PBP2. In the evolved REL1158A clone, which was isolated after 2,000 generations from population Ara+1 but still carried the ancestral $pbpA_{anc}$ allele, the PBP2 level was also similar to that in REL606 (Fig. 2B). Thus, both evolved *pbpA* alleles reduced the level of PBP2 compared to the ancestral allele. The results obtained with the transcriptional fusions indicate that this change occurred at the level of transcription. The two populations therefore evolved so that there were similar phenotypic changes in PBP2 expression that reflected the parallel substitution of mutations within the *pbpA* operon.

Evolved *pbpA* alleles change cell morphology. Given that the presence of the evolved *pbpA* alleles resulted in substantially reduced levels of PBP2, we first sought to assess whether the remaining PBP2 molecules were still functional in the evolved clones. Previous studies have reported that cells grow as enlarged spheres that eventually lyse when the transpeptidase activity of PBP2 is inhibited by amdinocillin (29, 65, 68). We therefore observed the effects of amdinocillin on cell morphology by using optical microscopy (Fig. 3A). Cultures of the ancestor strain REL606 and two evolved clones, REL1158C

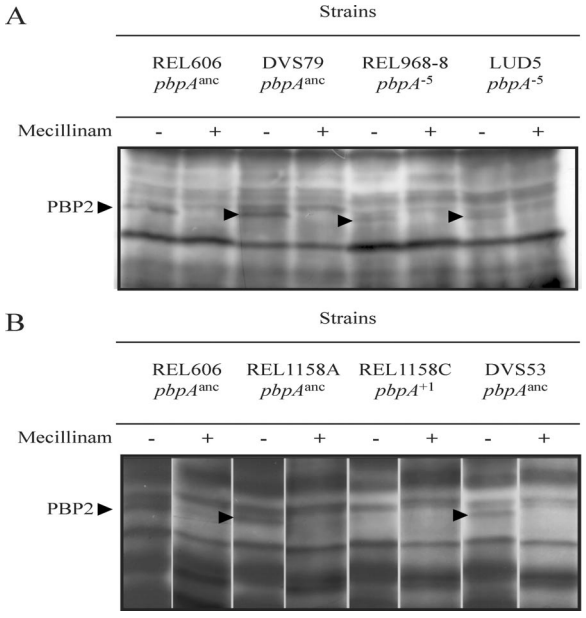

FIG. 2. Effects of *pbpA* mutations from populations Ara-5 (A) and Ara+1 (B) on the amount of PBP2. Strains were grown in DM250, and cells were collected upon entry into stationary phase. Membrane proteins were extracted, treated or not treated with 10 μM amdinocillin (Mecillinam), and incubated with fluorescein-conjugated ampicillin that bound to PBPs. Immunodetection was performed using 40-μg samples and antifluorescein antibodies. Competition between amdinocillin and ampicillin for binding to PBP2 allowed detection of PBP2 by comparison of samples treated with amdinocillin and samples not treated with amdinocillin (arrowheads). The following strains were used: REL606, the ancestor ($pbpA_{anc}$); REL968-8, a 1,000-generation clone from population Ara-5 carrying the evolved allele $pbpA_{-5}$; DVS79, same as REL968-8 except with $pbpA_{anc}$; LUD5, same as REL606 except with $pbpA_{-5}$; REL1158A, a 2,000-generation clone from population Ara+1 with the ancestral allele ($pbpA_{anc}$); REL1158C, another 2,000-generation clone from population Ara+1 but carrying the evolved allele $pbpA_{+1}$; and DVS53, same as REL1158C except with $pbpA_{anc}$.

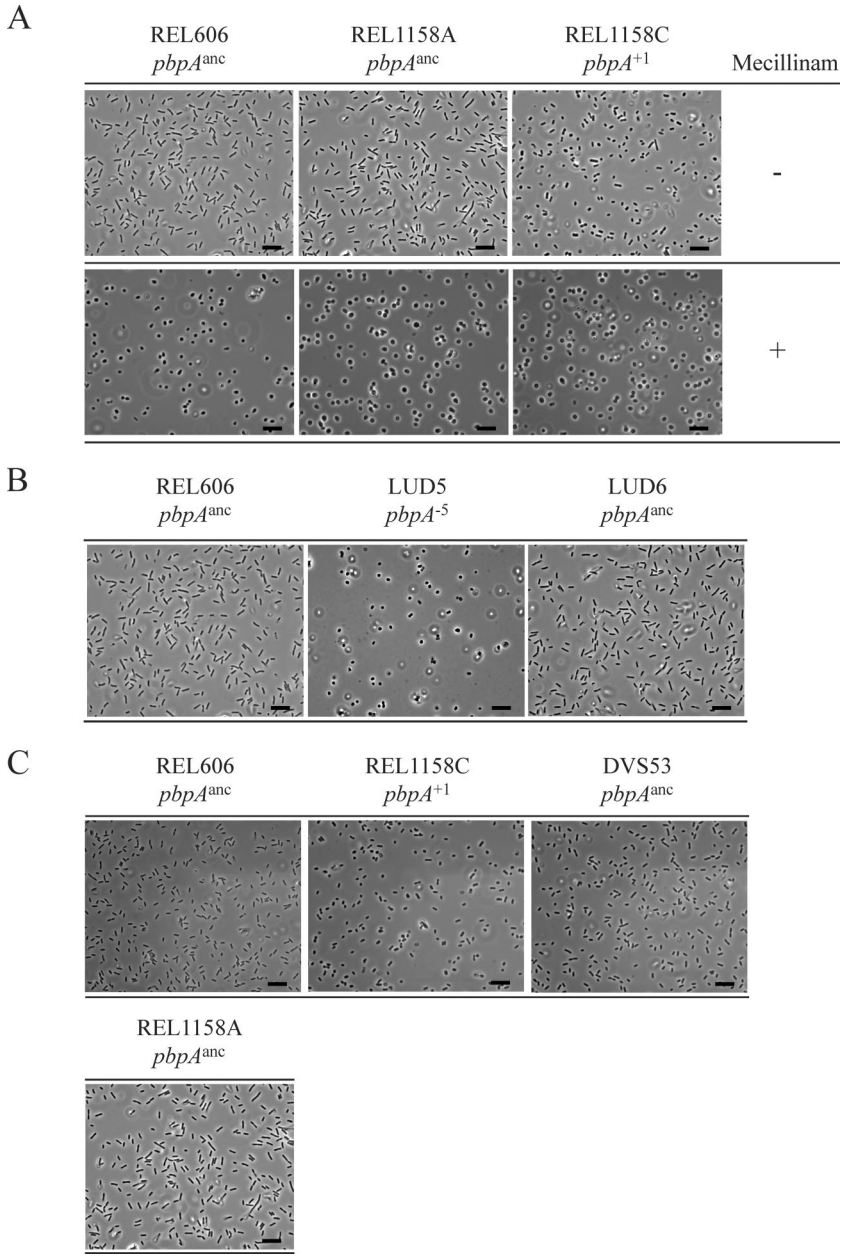

FIG. 3. Effects of evolved mutations in the *pbpA* operon on cell morphology. Cells were grown in DM250 with or without amdinocillin (Mecillinam) and observed using a Zeiss Axioplan 2 microscope. All photographs were obtained using a magnification of ×1,000, and all images are at the same relative scale. Bars = 10 μm. (A) Effects of inhibition of PBP2 activity with amdinocillin on cell shape. Strains were grown in DM250 for 1 h, and cultures were then split into two halves. One half was treated with amdinocillin (4 μg/ml) and incubated for an additional 5 h, and then cells were collected and observed. (B) Effect of evolved *pbpA* allele on cell morphology in population Ara-5. (C) Effect of evolved *pbpA* allele on cell morphology in population Ara+1. The following strains were used: REL606, the ancestor ($pbpA_{anc}$); REL1158A, a 2,000-generation clone from population Ara+1 with the ancestral allele ($pbpA_{anc}$); REL1158C, a 2,000-generation clone from population Ara+1 with the evolved allele $pbpA_{+1}$; LUD5, same as REL606 except with evolved allele $pbpA_{-5}$ from population Ara-5; LUD6, same as LUD5 except with $pbpA_{anc}$ restored; and DVS53, same as REL1158C except with $pbpA_{anc}$.

and REL1158A, both isolated at generation 2000 from population Ara+1 but carrying the $pbpA_{+1}$ and $pbpA_{anc}$ alleles, respectively, were treated with 4 μg/ml of amdinocillin and compared microscopically with untreated control cultures (Fig. 3A). The REL1158C cells clearly had a different shape than the cells of the two other strains, but in all cases the addition of amdinocillin led to enlarged spherical cells, which reflected the inhibition of cell wall elongation. This effect indicates that PBP2 remains functional even when the evolved $pbpA_{+1}$ allele is present.

We also analyzed the direct effects of the evolved *pbpA* mutations on cell shape. Cultures of the isogenic strains were sampled during exponential growth in DM250 (OD_{600}, 0.2), and cells were observed microscopically (Fig. 3B and C). The

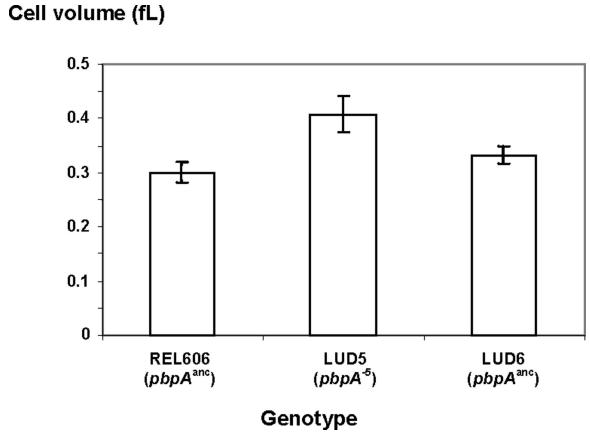

FIG. 4. Effect of evolved $pbpA_{-5}$ mutation on cell volume. Strains REL606 ($pbpA_{anc}$), LUD5 (same as REL606 except with evolved allele $pbpA_{-5}$), and LUD6 (LUD5 with the ancestral allele $pbpA_{anc}$ restored) were grown in DM25 under the conditions used in the long-term experiment and then diluted 1:100 in isotone solution (Beckman), and thousands of cell volumes were measured electronically using a Coulter Multisizer 3 counter (Beckman). The error bars indicate standard errors based on six replicate cultures for each strain.

cells of ancestral strain REL606 had the typical rod-shaped morphology of *E. coli* cells. However, the presence of both evolved *pbpA* alleles resulted in spherical cells, based on three lines of evidence. First, introduction of the $pbpA_{-5}$ allele into the ancestral chromosome led to spherical cells (strain LUD5), while restoring the ancestral allele (strain LUD6) restored the rod-shaped morphology (Fig. 3B). Second, the cells of an evolved clone (REL1158C) obtained from population Ara+1 at 2,000 generations and bearing $pbpA_{+1}$ were spherical, while introduction of $pbpA_{anc}$ (strain DVS53) resulted in morphology closer to the rod-shaped morphology typical of the ancestor (Fig. 3C). Also, individual cells of the evolved clone REL1158C were quite heterogeneous in terms of size, and introduction of the ancestral *pbpA* allele made them much less variable in this respect. Third, another evolved clone (REL1158A) isolated at 2,000 generations from population Ara+1 but still bearing the ancestral *pbpA* operon produced rod-shaped cells similar to the cells of the ancestor. Thus, both evolved *pbpA* alleles seem to disrupt cell wall elongation during exponential growth, as previously described for impairment of PBP2 activity (18). While this effect is well supported, replacement of the evolved allele by the ancestral allele in REL1158C did not result in precisely the same cell morphology as the ancestral strain, which indicates that one or more other mutations (at present unknown) had an effect in this evolved clone.

We also measured the average cell volume in stationary-phase cultures (after 24 h of incubation in DM25) for strains REL606, LUD5, and LUD6 using a Coulter counter (Fig. 4). The $pbpA_{-5}$ mutation increased the average volume by about 36%, and this phenotype was reversed in LUD6 (Fig. 4). The $pbpA_{-5}$ allele was first detected at 1,000 generations in population Ara-5 (see below). At that time, the average cell volume in the population was 0.630 fl (36), while introduction of the $pbpA_{-5}$ allele into the ancestral genome resulted in an average volume of 0.408 fl (Fig. 4). Therefore, while the $pbpA_{-5}$ allele had a large effect on cell volume, there were other mutations in population Ara-5 that also increased cell size.

Evolved *pbpA* alleles increase sensitivity to osmotic stress. The peptidoglycan layer plays an important role in protecting cells against osmotic pressure. Given that the evolved *pbpA* alleles lower the expression of PBP2, we measured the susceptibility of the ancestral and evolved cells to osmotic stress. Strains REL606, LUD5, LUD6, REL1158A, REL1158C, and DVS53 were grown in LB media containing a range of NaCl concentrations, and the net growth of each strain, reflecting differences in both growth and survival, was estimated by comparing viable cell counts to the counts for corresponding cultures without NaCl (Fig. 5). Introduction of the $pbpA_{-5}$ allele into the ancestral chromosome (strain LUD5) made the cells much more sensitive to osmotic stress, and this phenotype was completely reversed by restoring the ancestral allele when LUD6 was produced (Fig. 5A). Similarly, the evolved strain REL1158C ($pbpA_{+1}$) was much more sensitive to high NaCl concentrations than REL606 ($pbpA_{anc}$), and restoration of the ancestral *pbpA* allele (strain DVS53) reduced the sensitivity to the ancestral level. Strain REL1158A, also isolated at generation 2000 from the Ara+1 population, still possessed the ancestral *pbpA* allele, and it exhibited the high ancestral resistance to osmotic stress (Fig. 5B). Thus, both evolved *pbpA* alleles increased the sensitivity of cells to osmotic stress.

Evolved *pbpA* alleles enhance fitness during the long-term experiment. The fitness effect of the evolved $pbpA_{-5}$ allele was measured by performing 6-day competition assays with the marked ancestral strain and LUD5 (the ancestor with the $pbpA_{-5}$ allele), using the same conditions that were used in the long-term evolution experiment (Fig. 6A). As a control, the unmarked ancestor REL606 was used in a competition experiment with its marked counterpart, REL607, and there was no discernible effect of the marker on relative fitness ($H_0 = 1$; $n = 6$; $t_s = 0.3217$; $P = 0.7607$, as determined by a two-tailed test). By contrast, the fitness of the ancestral strain with the evolved $pbpA_{-5}$ allele, LUD5, relative to the marked ancestor, REL607, was 1.0441, and this effect was highly significant ($H_0 = 1$; $n = 6$; $t_s = 9.7148$; $P = 0.0001$, as determined by a one-tailed test). Moreover, this fitness advantage was eliminated when the $pbpA_{anc}$ allele was restored to produce strain LUD6 ($H_0 = 1$; $n = 6$; $t_s = 0.0141$; $P = 0.9893$, as determined by a two-tailed test), demonstrating that the benefit was specific to the $pbpA_{-5}$ allele.

To evaluate the fitness effect of the $pbpA_{+1}$ allele, strains REL607, REL1158C, and DVS53 were each used in competition experiments with the ancestral strain REL606 (Fig. 6B); again, the environment was the same one that was used for the long-term evolution experiment, but the assays lasted only 1 day because of the larger differences in fitness among some of these strains. REL607 is the progenitor of population Ara+1, REL1158C is a 2,000-generation clone of this population that carries the evolved $pbpA_{+1}$ allele, and DVS53 was constructed from REL1158C by introducing the $pbpA_{anc}$ allele. Once again, there was no significant difference between the marked ancestral variants ($H_0 = 1$; $n = 6$; $t_s = 0.3311$; $P = 0.7540$, as determined by a two-tailed test). The evolved clone REL1158C had a significant fitness advantage (1.243) relative to the ancestor ($H_0 = 1$; $n = 5$; $t_s = 15.0853$; $P < 0.0001$, as determined by a one-tailed test), which reflected not only the $pbpA_{+1}$ allele

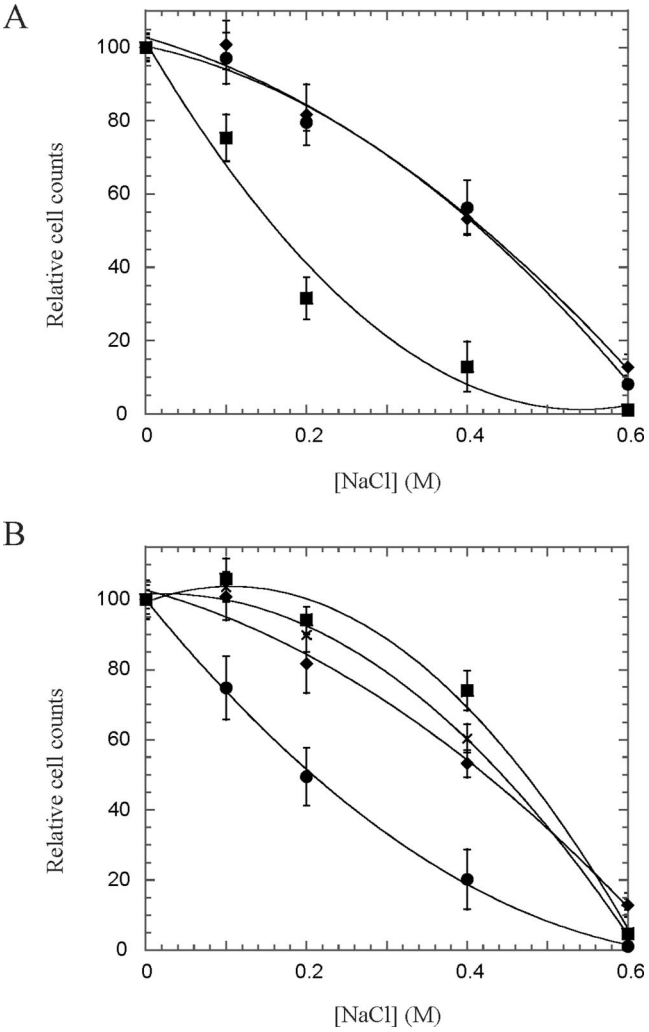

FIG. 5. Effects of the evolved *pbpA* alleles from populations Ara-5 (A) and Ara+1 (B) on sensitivity to osmotic stress. Each strain was grown in liquid LB media containing different NaCl concentrations for 12 h and then plated onto LB agar. The net population growth of each strain, reflecting the effects of NaCl on growth and survival, is expressed relative to the growth of cultures of the same strain in LB medium without NaCl. The error bars indicate standard errors based on four replicates for each combination of strain and NaCl concentration. (A) ◆, ancestral strain REL606 ($pbpA_{anc}$); ■, LUD5, same as REL606 except with evolved allele $pbpA_{-5}$ from population Ara-5; ●, LUD6, LUD5 with the ancestral allele $pbpA_{anc}$ restored. (B) ◆, REL606; ■, REL1158A, a 2,000-generation clone from population Ara+1 with the ancestral allele ($pbpA_{anc}$); ●, REL1158C, a 2,000-generation clone from population Ara+1 with the evolved allele ($pbpA_{+1}$); ×, DVS53, same as REL1158C except with the ancestral allele $pbpA_{anc}$.

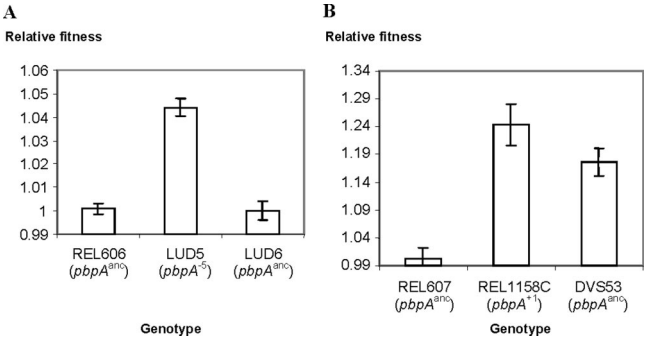

FIG. 6. Fitness effects of the evolved *pbpA* alleles. Competition assays were performed under the conditions used in the long-term evolution experiment, in all cases with the ancestor bearing the opposite Ara marker. The error bars indicate the 95% confidence intervals based on five or six replicate assays. Note the difference in scale between the two panels. (A) Population Ara-5. The following strains were used: REL606, the Ara$^-$ ancestor ($pbpA_{anc}$); LUD5, same as the ancestor except with the evolved allele $pbpA_{-5}$; and LUD6, strain LUD5 with the ancestral allele $pbpA_{anc}$ restored. (B) Population Ara+1. The following strains were used: REL607, the Ara$^+$ ancestor ($pbpA_{anc}$); REL1158C, clone from generation 2000 with the evolved allele $pbpA_{+1}$; and DVS53, same as clone REL1158C except with the ancestral allele $pbpA_{anc}$ introduced.

but also all other beneficial mutations that occurred during its 2,000 generations of evolution. As expected for these other beneficial substitutions, the isogenic construct DVS53, which possesses the evolved genome except for the *pbpA* allele, also had a significant, albeit smaller, fitness advantage (1.176) relative to the ancestor ($H_0 = 1$; $n = 5$; $t_s = 18.0391$; $P < 0.0001$, as determined by a one-tailed test). Importantly, the difference in fitness between REL1158C and DVS53, which reflected the specific effect of the $pbpA_{+1}$ allele, was itself very significant ($H_0 = 0$; $t_s = 3.5574$; $P = 0.0037$, as determined by a one-tailed test). Thus, both evolved *pbpA* alleles were beneficial in the environment used for the long-term evolution experiment, indicating that a reduced level of PBP2 is advantageous under these conditions.

To investigate the origin and subsequent dynamics of substitution of the evolved *pbpA* alleles, we analyzed (as described in Materials and Methods) the corresponding genomic region in many clones obtained from populations Ara-5 and Ara+1 between generations 500 and 2000. The evolved *pbpA* allele was not detected at generation 500 in population Ara-5, but it was present in ~90% of the clones sampled at generation 1000 and in all of the clones from generation 2000 (Table 3). In population Ara+1, the evolved *pbpA* allele was not detected at generation 500 or 1000, but it was present in ~30 and ~90% of the clones tested from generations 1500 and 2000, respectively (Table 3). Thus, both mutations contributed to the large early gains in fitness (36), and both mutations were transiently polymorphic before they were fixed in their respective populations.

TABLE 3. Dynamics of the evolved *pbpA* alleles in populations Ara-5 and Ara+1

Generation	No. of clones with $pbpA_{-5}$/ total no.[a]	No. of clones with $pbpA_{+1}$/ total no.[b]
500	0/18	0/50
1,000	16/18	0/50
1,500	ND[c]	15/50
2,000	18/18	44/49

[a] For population Ara-5, PCR products were tested by examining enzymatic restriction with GsuI.

[b] For population Ara+1, the size of the PCR product indicated whether the ancestral or evolved allele was present.

[c] ND, not determined.

Evolved $pbpA_{-5}$ allele reduces fitness during prolonged stationary phase. In a recent study, another PBP, PBP1b, was shown to be necessary for survival during prolonged nutritional stress (51). The role of PBP2 under these conditions was not investigated in the previous study because the loss of PBP2 is lethal in rich medium. However, we were able to perform competition experiments using isogenic strains to examine the effect of *pbpA* expression on the survival of cells during prolonged starvation.

We performed competition experiments in which each of three strains, REL606 ($pbpA_{anc}$), LUD5 (REL606 except with the evolved $pbpA_{-5}$ allele), and LUD6 (LUD5 except with the $pbpA_{anc}$ allele restored), was grown with REL607 in LB medium (without serial transfer) for 15 days. Spontaneous nalidixic acid resistance mutations were used as an additional marker to distinguish competitors, and the marker was switched between the competitors to confirm that it did not affect the outcome. After 15 days, LUD5 was completely outcompeted by REL607, and the LUD5 level was below the limit of detection (~10 cells per ml) in all six replicates (three replicates with each resistance marker state). By contrast, REL606 and LUD6 each persisted along with REL607 in all six replicates, and the average ratios were similar to the starting ratio. Thus, LUD5, which carried the evolved $pbpA_{-5}$ allele, exhibited the stationary-phase-specific competition-defective phenotype (51), while its otherwise isogenic counterparts with the ancestral *pbpA* allele did not. No differences between the strains grown as monocultures were detected. PBP2 evidently has an important physiological role in promoting competitiveness and survival during prolonged nutrient deprivation.

DISCUSSION

We examined the fitness and other phenotypic consequences of mutations affecting the *pbpA* operon that were substituted during a long-term evolution experiment in a glucose-limited minimal medium (61, 79). Statistical analyses, including analyses of parallel substitutions of mutations in *pbpA* in 6 of 12 lines, suggested that these mutations were beneficial (79), an inference that is directly supported by our study. In particular, we analyzed two of these mutations, the mutations substituted in populations Ara+1 and Ara-5 and located in the putative transcriptional regulatory region of the operon (2, 61, 79). We constructed isogenic strains that differ only in the presence of the ancestral or evolved *pbpA* alleles. Both evolved mutations decreased transcription of the *pbpA* operon, resulting in smaller amounts of PBP2. The reduced levels of PBP2 led to changes in cell morphology, giving rise to coccoid cells with increased volume. Competition experiments with the isogenic strains demonstrated that both mutations improved fitness in the seasonal environment used for the long-term experiment, in which populations experience daily cycles of feast and famine. Both *pbpA* mutations arose during the first 2,000 generations of the long-term experiment, which corresponded to the period of most rapid fitness gains.

The evolved *pbpA* mutations also had pleiotropic effects that were detrimental under certain other conditions. In particular, both evolved *pbpA* alleles caused increased sensitivity to osmotic stress. We also showed that the evolved $pbpA_{-5}$ allele reduced competitive performance during prolonged starvation over many days. The disadvantage during starvation might be related to observations made in two previous studies. First, the inhibition of PBP2 by amdinocillin has been reported to delay the initiation of both peptidoglycan synthesis and growth when cells are in stationary phase (16). However, the populations in the long-term experiment evolved a shorter lag phase after the daily transfers into fresh medium (74). Any physiological effect that delayed the transition between the stationary and growth phases would have been detrimental during the experiment, and therefore it seems unlikely that such an effect is associated with the evolved *pbpA* alleles. Second, stationary-phase cells retained significant peptidoglycan biosynthetic activity involving PBP2 (7), and this continued activity may have imposed a cost under the conditions of the long-term experiment. By reducing PBP2 activity to avoid this cost, the viability of the cells during prolonged starvation might have been compromised. In any case, PBP2 is likely involved in the turnover of murein during stationary phase and in the initiation of murein synthesis during regrowth, and both of these processes are undoubtedly important for success in the seasonal feast-and-famine environment of the long-term experiment. The evolved *pbpA* alleles are clearly beneficial in the selective environment in which they arose, but they are deleterious under some other conditions, thus indicating that there is a trade-off. Trade-offs have also been reported for two other loci that also underwent parallel substitutions in the long-term lines, in particular, beneficial mutations in the *rbs* operon (12) and the *malT* gene (50) led to decay of unused ribose and maltose catabolic functions, respectively.

It is important to emphasize that our molecular studies focused on the expression of *pbpA*. However, the *pbpA* gene is in an operon that includes three other genes; two of these genes, *ybeB* and *ybeA*, have unknown functions (2), and *rodA* encodes a protein required for PBP2 function and is involved in maintenance of the rod-shaped cell morphology (18). Previous research has shown that alterations to RodA and PBP2 can have similar phenotypic effects (18). Another gene, *rlpA*, encoding one of two rare lipoproteins (69), may also belong to the same operon (56), and its function is unknown except that a truncated version of RlpA suppresses a null mutant of the *prc*-encoded periplasmic protease (3). The *dacA* gene, which encodes PBP5 and thus is also involved in peptidoglycan biosynthesis (45), is immediately downstream of the *pbpA* operon. However, neither the Ara+1 nor the Ara-5 evolved allele affects the amount of PBP5 (data not shown), indicating that *dacA* is probably not part of the same operon. By reducing transcription, the evolved *pbpA* alleles may affect the levels of all proteins encoded by the operon. We did not measure the amounts of RodA or the other proteins encoded by genes in the operon because of the lack of suitable antibodies. However, sequencing of the operon (except *rlpA*) in clones obtained from the 12 populations revealed mutations in the promoter region and in *pbpA* but not in any of the other genes (79). Several studies have documented that there is a high level of genetic parallelism underlying adaptation in these populations (11, 12, 50, 79), and therefore we hypothesized that the increased fitness and other changes associated with the mutations affecting the *pbpA* operon reflect the altered level of PBP2 itself. We attempted to check this hypothesis directly by introducing into the ancestral strain a mutation substituted in

another population (Ara-1) (Fig. 1) that affected the coding region of *pbpA*. However, despite multiple efforts, this experiment was unsuccessful. Hence, we cannot exclude the possibility that changes in the amounts of YbeB, YbeA, RodA, and RlpA also contribute to the improved fitness and other phenotypic effects of the evolved alleles.

We showed that both the Ara-5 and Ara+1 mutations reduce the transcription of *pbpA*. Both mutations are located upstream of the translational start of *ybeB*, the first gene in the operon. A putative promoter has been identified upstream of the operon (2). The Ara+1 mutation is an IS*150* insertion that is only 11 bp upstream of the −35 box of this putative promoter and may directly affect its transcriptional activity. The Ara-5 allele harbors a point mutation 95 bp downstream of the −35 box position. Although this mutation clearly also decreases transcription, the underlying mechanism is not known. Some possible mechanisms include the presence of additional promoters, binding sites for regulatory proteins, or genes for noncoding RNAs. Interestingly, two other mutations in another population, designated Ara-2, also affect this region and are located 22 and 153 bp downstream of the −35 box position. Thus, analyses of these evolved alleles may reveal a regulatory region for the *ybeBA-rodA-pbpA-rlpA* operon that is more complex than previously recognized. This complexity may allow differential regulation of these genes and thus contribute to the dynamic behavior of the peptidoglycan structure (71).

PBP2 is well characterized biochemically and has been shown to have DD-transpeptidase activity in vitro (28). PBP2 and other PBPs are involved in the assembly of peptidoglycan by giving the glycan chains their structural integrity. Impairment of PBP2 activity leads to spherical cells instead of the rod-shaped morphology typical of *E. coli* (4). In good agreement with previous work, our experiments demonstrated that both evolved alleles simultaneously reduce the amount of PBP2 and result in cells that are more spherical. Despite substantial information at the biochemical level, however, the precise functions of many PBPs, including PBP2, are less clear. In particular, there is substantial functional redundancy among PBPs in *E. coli*; mutant strains with only one PBP impaired often have no obvious phenotypes (81), and even a mutant deficient in 8 of the 12 PBPs was viable (17). PBP5 has been shown to influence the diameter, contour, and shape of *E. coli* cells (45), but these effects are much more visible in mutants lacking other PBPs as well as PBP5. This apparent redundancy suggests that most PBPs are not essential under standard laboratory conditions, although they may have greater physiological relevance in other environments. Consistent with this view, PBP1a influences the synthesis of the colonic acid capsule and temperature sensitivity, while PBP1a and PBP5 may contribute to phage resistance (81). Also, PBP1b has been shown to be important to *E. coli* cells during prolonged stationary phase, whereas nine other PBPs were dispensable under these conditions (51), although this study did not include PBP2. All of these previous studies analyzed deliberately constructed knockout and other mutants with mutations in the various PBP-encoding genes. By contrast, we analyzed two *pbpA* alleles that evolved and were beneficial to *E. coli*, albeit under benign conditions. We showed that both mutations decrease the level of PBP2 while they increase the sensitivity to osmotic stress and, in at least one case, reduce fitness during prolonged starvation, implying that this protein has important stress-related functions that are, however, costly to maintain when they are not needed.

This pattern of trade-offs between increased fitness in the selective environment and reduced performance under certain other conditions implies that there is ecological specialization (13). Two population genetic processes, mutation accumulation and antagonistic pleiotropy, can produce this specialization. Mutation accumulation involves the spread by random drift, hitchhiking, or both of mutations that are neutral or even slightly deleterious, such as mutations in the genes that encode pathways that are not used in the selective environment. In contrast, antagonistic pleiotropy is driven by natural selection and occurs when mutations that are beneficial in the selective environment have deleterious side effects on performance under other conditions. Cooper and Lenski (13) described several lines of evidence indicating that antagonistic pleiotropy was more important than mutation accumulation in the long-term experiment with *E. coli*. However, a direct genetic test would require demonstrating that the same mutations are responsible for both adaptation and increased specialization. By constructing isogenic strains that differ only in whether they possess an ancestral or evolved *pbpA* allele, we showed that the *pbpA* mutations are beneficial in the benign environment where they evolved and deleterious under certain more stressful conditions, thereby providing direct evidence for antagonistic pleiotropy. Direct support for antagonistic pleiotropy was also obtained in two previous studies with the long-term lines, which showed that mutations that were beneficial in the glucose environment resulted in a diminished capacity to grow on ribose and maltose (12, 50). Reductions in the costs of expressing unused functions may explain the benefits associated with these mutations, although indirect effects might also be important (22). In any case, ecological specialization caused by antagonistic pleiotropy is not restricted to catabolic abilities in these populations. Such trade-offs also imply that selection may favor a fine-tuned balance between the benefits and costs associated with a given protein (15). In this context, it is noteworthy that PBP2 is one of the less abundant PBPs in *E. coli*, with only ~100 molecules per cell (21, 67), yet it evolved to an even lower concentration in at least some of the long-term lines under a selective regimen that strongly favors rapid growth (74). Based on differences in the intensity of the PBP2 bands in Fig. 2, we estimated that the ancestral allele yields roughly fivefold more protein than either of the evolved *pbpA* alleles.

Impairment of PBP2 activity leads to spherical cells in which peptidoglycan is largely confined to the septum (18), which may limit peptidoglycan recycling (72). Consistent with this, the evolved *pbpA* alleles reduce PBP2 levels while also generating spherical cells. The fitness advantage conferred by the evolved *pbpA* alleles in a glucose environment might reflect the reduced cost of maintaining the cell wall elongation function more generally (i.e., beyond the energetic savings associated with lower PBP2 levels per se). Many PBPs are part of multienzyme complexes (59) that interact with one another (6) or with peptidoglycan hydrolases (32, 55, 77), and the interactions may coordinate the hydrolysis of peptidoglycan and the introduction of new cell wall material during the cell cycle. Many PBPs also interact with other proteins, including MreC, which

is an essential protein involved in determining cell shape that is encoded by the *mreBCD* operon (20). This operon also encodes MreB, an actin homolog that forms helical filaments beneath the inner membrane along the cell length. PBP2, in particular, has been shown to interact with MreC in both *Caulobacter crescentus* (20) and *Bacillus subtilis* (73) and with other PBPs in *C. crescentus* (23). PBP2 may also occur in the multiprotein membrane-bound complexes involved in lateral peptidoglycan biosynthesis (30). The MreB filaments might spatially organize the PBPs within the inner membrane, thereby maintaining cell shape, in part by structuring the PBP2-peptidoglycan biosynthesis complex (23). In this way MreB may help coordinate the switch from longitudinal to septal peptidoglycan synthesis during cell division, which is particularly relevant in *E. coli* because PBP2 directs cell elongation, whereas PBP3 redirects most peptidoglycan synthesis to the septum (19). Although many details of these interactions remain unclear, it seems likely that changes in the concentration of PBP2 could have important effects on this complex network of interacting proteins.

All 12 populations in the long-term experiment evolved cells that were much larger, on average, as they became more fit (36), and in several populations the cells also became more spherical (35). As a consequence of the increased size and altered shape, the average ratio of surface area to volume declined in the evolved bacteria relative to the ratio for their common ancestor (35). We have demonstrated that mutations in the *pbpA* operon contribute to these phenotypic changes in two populations, and four other populations also have mutations in the *pbpA* operon (79) that likely influence cell size and shape as well. However, other mutations must also contribute to the changes in cell morphology because in all 12 populations the average cell size increased and because the *pbpA* mutations that we studied explain only a small portion of the overall increase in average cell volume in the populations where they arose.

Moreover, the selective advantage or other explanation for the evolved changes in cell size and shape, including the lower ratio of surface area to volume, remains unclear. However, below we offer a few hypotheses, as well as some evidence that bears on them. It has long been known that fast-growing cells are larger than slow-growing cells (1, 58). Hence, one nonadaptive explanation is that the evolved bacteria produce larger cells simply as a correlated effect of their faster growth. However, this explanation was rejected by showing that the evolved bacteria produced larger cells than the ancestor even when both types of bacteria were forced to grow at the same rate by placing them in separate chemostats at the same dilution rate (43). Also, the lower surface-to-volume ratio of the evolved cells seems to be maladaptive in a nutrient-limited environment, although one could hypothesize that there are certain advantages in the context of the daily serial transfer regimen under which the populations evolved. In particular, larger cells have more reserves that might allow them to commence growth more quickly upon transfer into fresh medium. Cells with larger absolute surface areas might also function as larger sponges, allowing them to accumulate glucose faster than they can use it, thereby provisioning their progeny with carbon and energy that they can use after the glucose has been depleted from the medium. Such a strategy might provide a competitive advantage specific to the feast-and-famine regimen imposed by serial transfer. Alternatively, a mathematical model of bacterial growth predicts that larger cells result if selection increases both the transport of the limiting nutrient into the cell and the efficiency of biomass conversion (25), without any direct selection on cell morphology per se. The rate of glucose transport presumably increased in the evolved bacteria, given their faster growth on glucose and the specificity of their fitness gains with respect to carbon sources that, like glucose, employ the phosphotransferase system (47, 70). Also, the reduced costs of maintaining unused functions have increased the efficiency with which the evolved bacteria convert the limiting glucose into biomass (35, 37, 46). For now, it is still unclear precisely why the evolved bacteria produce larger cells than their ancestors, but the mutations in the *pbpA* operon that we studied here contribute simultaneously to the improved fitness, increased volume, and altered shape in some of the lineages.

ACKNOWLEDGMENTS

Our collaborative research was supported by Université Joseph Fourier, by Centre National de la Recherche Scientifique, by the Agence Nationale de la Recherche (ANR) program "Biologie Systémique (BIOSYS)," by Michigan State University, by the National Science Foundation, and by the DARPA "FunBio" program. N.P. acknowledges the Ministry of Education Nationale de l'Enseignement Supérieur et de la Recherche for providing a research fellowship and the Université Joseph Fourier for providing ATER funding. L.P. acknowledges the Centre National de la Recherche Scientifique for providing a postdoctoral fellowship.

We thank other members of our research groups and outside collaborators for many contributions to this work. We thank Laboratories Léo (France) for the gift of amdinocillin and Galleni Moreno (University of Liège, Liège, Belgium) for providing the fluorescein-conjugated ampicillin. We thank Pam MacDonald (University of California, Irvine) for technical assistance with measuring cell sizes and Al Bennett for allowing us to use equipment for these measurements.

REFERENCES

1. **Åkerlund, T., K. Nordström, and R. Bernander.** 1995. Analysis of cell size and DNA content in exponentially growing and stationary-phase batch cultures of *Escherichia coli*. J. Bacteriol. **177:**6791–6797.
2. **Asoh, S., H. Matsuzawa, F. Ishino, J. L. Strominger, M. Matsuhashi, and T. Ohta.** 1986. Nucleotide sequence of the *pbpA* gene and characteristics of the deduced amino acid sequence of penicillin-binding protein 2 of *Escherichia coli* K12. Eur. J. Biochem. **160:**231–238.
3. **Bass, S., Q. Gu, and A. Christen.** 1996. Multicopy suppressors of Prc mutant *Escherichia coli* include two HtrA (DegP) protease homologs (HhoAB), DksA, and a truncated RlpA. J. Bacteriol. **178:**1154–1161.
4. **Begg, K. J., and W. D. Donachie.** 1985. Cell shape and division in *Escherichia coli*: experiments with shape and division mutants. J. Bacteriol. **163:**615–622.
5. **Begg, K. J., and W. D. Donachie.** 1998. Division planes alternate in spherical cells of *Escherichia coli*. J. Bacteriol. **180:**2564–2567.
6. **Bertsche, U., T. Kast, B. Wolf, C. Fraipont, M. E. G. Aarsman, K. Kannenberg, M. von Rechenberg, M. Nguyen-Distèche, T. den Blaauwen, J.-V. Höltje, and W. Vollmer.** 2006. Interaction between two murein (peptidoglycan) synthases, PBP3 and PBP1B, in *Escherichia coli*. Mol. Microbiol. **61:**675–690.
7. **Blasco, B., A. G. Pisabarro, and M. A. De Pedro.** 1988. Peptidoglycan biosynthesis in stationary-phase cells of *Escherichia coli*. J. Bacteriol. **170:**5224–5228.
8. **Bledig, S. A., T. M. Ramseier, and M. H. Saier, Jr.** 1996. FruR mediates catabolite activation of pyruvate kinase (*pykF*) gene expression in *Escherichia coli*. J. Bacteriol. **178:**280–283.
9. **Blount, Z. D., C. Z. Borland, and R. E. Lenski.** 2008. Historical contingency and the evolution of a key innovation in an experimental population of *Escherichia coli*. Proc. Natl. Acad. Sci. USA **105:**7899–7906.
10. **Botta, G. A., and J. T. Park.** 1981. Evidence for involvement of penicillin binding protein 3 in murein synthesis during septation but not during cell elongation. J. Bacteriol. **145:**333–340.
11. **Cooper, T. F., D. E. Rozen, and R. E. Lenski.** 2003. Parallel changes in gene

expression after 20,000 generations of evolution in *Escherichia coli*. Proc. Natl. Acad. Sci. USA **100:**1072–1077.
12. **Cooper, V. S., D. Schneider, M. Blot, and R. E. Lenski.** 2001. Mechanisms causing rapid and parallel losses of ribose catabolism in evolving populations of *Escherichia coli* B. J. Bacteriol. **183:**2834–2841.
13. **Cooper, V. S., and R. E. Lenski.** 2000. The population genetics of ecological specialization in evolving *Escherichia coli* populations. Nature **407:**736–739.
14. **Crozat, E., N. Philippe, R. E. Lenski, J. Geiselmann, and D. Schneider.** 2005. Long-term experimental evolution in *Escherichia coli*. XII. DNA topology as a key target of selection. Genetics **169:**523–532.
15. **Dekel, E., and U. Alon.** 2005. Optimality and evolutionary tuning of the expression level of a protein. Nature **436:**588–592.
16. **de la Rosa, E. J., M. A. de Pedro, and D. Vazquez.** 1985. Penicillin binding proteins: role in initiation of murein synthesis in *Escherichia coli*. Proc. Natl. Acad. Sci. USA **82:**5632–5635.
17. **Denome, S. A., P. K. Elf, T. A. Henderson, D. E. Nelson, and K. D. Young.** 1999. *Escherichia coli* mutants lacking all possible combinations of eight penicillin binding proteins: viability, characteristics, and implications for peptidoglycan synthesis. J. Bacteriol. **181:**3981–3993.
18. **de Pedro, M. A., W. D. Donachie, J. V. Holtje, and H. Schwarz.** 2001. Constitutive septal murein synthesis in *Escherichia coli* with impaired activity of the morphogenetic proteins RodA and penicillin-binding protein 2. J. Bacteriol. **183:**4115–4126.
19. **de Pedro, M. A., J. C. Quintala, J. V. Höltje, and H. Schwartz.** 1997. Murein segregation in *Escherichia coli*. J. Bacteriol. **179:**2823–2834.
20. **Divakaruni, A. V., R. R. Ogorzalek Loo, Y. Xie, J. A. Loo, and J. W. Gober.** 2005. The cell-shape protein MreC interacts with extracytoplasmic proteins including cell wall assembly complexes in *Caulobacter crescentus*. Proc. Natl. Acad. Sci. USA **102:**18602–18607.
21. **Dougherty, T. J., K. Kennedy, R. E. Kessler, and M. J. Pucci.** 1996. Direct quantitation of the number of individual penicillin-binding proteins per cell in *Escherichia coli*. J. Bacteriol. **178:**6110–6115.
22. **Dykhuizen, D.** 1978. Selection for tryptophan auxotrophs of *Escherichia coli* in glucose-limited chemostats as a test of the energy conservation hypothesis of evolution. Evolution **32:**125–150.
23. **Figge, R. M., A. V. Divakaruni, and J. W. Gober.** 2004. MreB, the cell shape-determining bacterial actin homologue, co-ordinates cell wall morphogenesis in *Caulobacter crescentus*. Mol. Microbiol. **51:**1321–1332.
24. **Goffin, C., and J. M. Ghuysen.** 1998. Multimodular penicillin-binding proteins: an enigmatic family of orthologs and paralogs. Microbiol. Mol. Biol. Rev. **62:**1079–1093.
25. **Graña, M., and L. Acerenza.** 2001. A model combining cell physiology and population genetics to explain *Escherichia coli* laboratory evolution. BMC Evol. Biol. **1:**12.
26. **Grose, J. H., U. Bergthorsson, and J. R. Roth.** 2005. Regulation of NAD biosynthesis by the trifunctional NadR protein of *Salmonella enterica*. J. Bacteriol. **187:**2774–2782.
27. **Huisman, G. W., D. A. Siegele, M. M. Zambrano, and R. Kolter.** 1996. Morphological and physiological changes during stationary phase, p. 1672–1682. *In* F. C. Neidhardt, R. Curtiss III, J. L. Ingraham, E. C. C. Lin, K. B. Low, B. Magasanik, W. S. Reznikoff, M. Riley, M. Schaechter, and H. E. Umbarger (ed.), *Escherichia coli* and *Salmonella*: cellular and molecular biology, 2nd ed. ASM Press, Washington, DC.
28. **Ishino, F., W. Park, S. Tomioka, S. Tamaki, I. Takase, K. Kunugita, H. Matsuzawa, S. Asoh, T. Ohta, and B. G. Spratt.** 1986. Peptidoglycan synthetic activities in membranes of *Escherichia coli* caused by overproduction of penicillin-binding protein 2 and RodA protein. J. Biol. Chem. **261:**7024–7031.
29. **James, R., J. Y. Haga, and A. B. Pardee.** 1975. Inhibition of an early event in the cell division cycle of *Escherichia coli* by FL1060, an amidinopenicillanic acid. J. Bacteriol. **122:**1283–1292.
30. **Kruse, T., J. Bork-Jensen, and K. Gerdes.** 2005. The morphogenetic MreBCD proteins of *Escherichia coli* form an essential membrane-bound complex. Mol. Microbiol. **55:**78–89.
31. **Lederberg, S.** 1966. Genetics of host-controlled restriction and modification of deoxyribonucleic acid in *Escherichia coli*. J. Bacteriol. **91:**1029–1036.
32. **Legaree, B. A., C. B. Adams, and A. J. Clarke.** 2007. Overproduction of penicillin-binding protein 2 and its inactive variants causes morphological changes and lysis in *Escherichia coli*. J. Bacteriol. **189:**4975–4983.
33. **Lenski, R. E.** 2004. Phenotypic and genomic evolution during a 20,000-generation experiment with the bacterium *Escherichia coli*. Plant Breed. Rev. **24:**225–265.
34. **Lenski, R. E., C. L. Winkworth, and M. A. Riley.** 2003. Rates of DNA sequence evolution in experimental populations of *Escherichia coli* during 20,000 generations. J. Mol. Evol. **56:**498–508.
35. **Lenski, R. E., and J. A. Mongold.** 2000. Cell size, shape, and fitness in evolving populations of bacteria, p. 221–235. *In* J. H. Brown and G. B. West (ed.), Scaling in biology. Oxford University Press, Oxford, United Kingdom.
36. **Lenski, R. E., and M. Travisano.** 1994. Dynamics of adaptation and diversification: a 10,000-generation experiment with bacterial populations. Proc. Natl. Acad. Sci. USA **91:**6808–6814.
37. **Lenski, R. E., J. A. Mongold, P. D. Sniegowski, M. Travisano, F. Vasi, P. J. Gerrish, and T. Schmidt.** 1998. Evolution of competitive fitness in experimental populations of *E. coli*: what makes one genotype a better competitor than another? Antonie van Leeuwenhoek **73:**35–47.
38. **Lenski, R. E., M. R. Rose, S. C. Simpson, and S. C. Tadler.** 1991. Long-term experimental evolution in *Escherichia coli*. I. Adaptation and divergence during 2000 generations. Am. Nat. **138:**1315–1341.
39. **Link, A. J., D. Phillips, and G. M. Church.** 1997. Methods for generating precise deletions and insertions in the genome of wild-type *Escherichia coli*: application to open reading frame characterization. J. Bacteriol. **179:**6228–6237.
40. **Macheboeuf, P., C. Contreras-Martel, V. Job, O. Dideberg, and A. Dessen.** 2006. Penicillin binding proteins: key players in bacterial cell cycle and drug resistance processes. FEMS Microbiol. Rev. **30:**673–691.
41. **McPherson, D. C., and D. L. Popham.** 2003. Peptidoglycan synthesis in the absence of class A penicillin-binding proteins in *Bacillus subtilis*. J. Bacteriol. **185:**1423–1431.
42. **Miller, J. H.** 1972. Experiments in molecular genetics. Cold Spring Harbor Laboratory Press, Cold Spring Harbor, NY.
43. **Mongold, J. A., and R. E. Lenski.** 1996. Experimental rejection of a nonadaptive explanation for increased cell size in *Escherichia coli*. J. Bacteriol. **178:**5333–5334.
44. **Nelson, D. E., and K. D. Young.** 2001. Contributions of PBP 5 and DD-carboxypeptidase penicillin binding proteins to maintenance of cell shape in *Escherichia coli*. J. Bacteriol. **183:**3055–3064.
45. **Nelson, D. E., and K. D. Young.** 2000. Penicillin binding protein 5 affects cell diameter, contour, and morphology of *Escherichia coli*. J. Bacteriol. **182:**1714–1721.
46. **Novak, M., T. Pfeiffer, R. E. Lenski, U. Sauer, and S. Bonhoeffer.** 2006. Experimental tests for an evolutionary trade-off between growth rate and yield in *E. coli*. Am. Nat. **168:**242–251.
47. **Ostrowski, E. A., R. J. Woods, and R. E. Lenski.** 2008. The genetic basis of parallel and divergent phenotypic responses in evolving populations of *Escherichia coli*. Proc. R. Soc. Lond. B **275:**277–284.
48. **Papadopoulos, D., D. Schneider, J. Meier-Eiss, W. Arber, R. E. Lenski, and M. Blot.** 1999. Genomic evolution during a 10,000-generation experiment with bacteria. Proc. Natl. Acad. Sci. USA **96:**3807–3812.
49. **Pedersen, K., and K. Gerdes.** 1999. Multiple *hok* genes on the chromosome of *Escherichia coli*. Mol. Microbiol. **32:**1090–1102.
50. **Pelosi, L., L. Kuhn, D. Guetta, J. Garin, J. Geiselmann, R. E. Lenski, and D. Schneider.** 2006. Parallel changes in global protein profiles during long-term experimental evolution in *Escherichia coli*. Genetics **173:**1851–1869.
51. **Pepper, E. D., M. J. Farrell, and S. E. Finkel.** 2006. Role of penicillin-binding protein 1b in competitive stationary phase survival of *Escherichia coli*. FEMS Microbiol. Lett. **263:**61–67.
52. **Philippe, N., E. Crozat, R. E. Lenski, and D. Schneider.** 2007. Evolution of global regulatory networks during a long-term experiment with *Escherichia coli*. BioEssays **29:**846–860.
53. **Popham, D. L., and K. D. Young.** 2003. Role of penicillin-binding proteins in bacterial cell morphogenesis. Curr. Opin. Microbiol. **6:**594–599.
54. **Powell, B. S., D. L. Court, Y. Nakamura, M. P. Rivas, and C. L. Turnbough, Jr.** 1994. Rapid confirmation of single copy lambda prophage integration by PCR. Nucleic Acids Res. **22:**5765–5766.
55. **Romeis, T., and J. V. Höltje.** 1994. Specific interaction of penicillin-binding proteins 3 and 7/8 with soluble lytic transglycosylase in *Escherichia coli*. J. Biol. Chem. **269:**21603–21607.
56. **Salgado, H., S. Gama-Castro, M. Paralta-Gil, E. Diaz-Peredo, F. Sanchez-Solano, A. Santos-Zavaleta, I. Martinez-Flores, V. Jimenez-Jacinto, C. Bonavides-Martinez, J. Segura-Salazar, A. Martinez-Antonio, and J. Collado-Vides.** 2006. RegulonDB (version 5.0): *Escherichia coli* K-12 transcriptional regulatory network, operon organization, and growth conditions. Nucleic Acids Res. **34:**D394–397.
57. **Sambrook, J., E. F. Fritsch, and T. Maniatis.** 1989. Molecular cloning: a laboratory manual, 2nd ed. Cold Spring Harbor Laboratory Press, Plainview, NY.
58. **Schaechter, M., O. Maaløe, and N. O. Kjelgaard.** 1958. Dependence on medium and temperature of cell size and chemical composition during balanced growth of *Salmonella typhimurium*. J. Gen. Microbiol. **19:**592–606.
59. **Schiffer, G., and J. V. Höltje.** 1999. Cloning and characterization of PBP 1C, a third member of the multimodular class A penicillin-binding proteins of *Escherichia coli*. J. Biol. Chem. **274:**32031–32039.
60. **Schneider, D., E. Duperchy, J. Depeyrot, E. Coursange, R. E. Lenski, and M. Blot.** 2002. Genomic comparisons among *Escherichia coli* strains B, K-12, and O157:H7 using IS elements as molecular markers. BMC Microbiol. **2:**18.
61. **Schneider, D., E. Duperchy, E. Coursange, R. E. Lenski, and M. Blot.** 2000. Long-term experimental evolution in *Escherichia coli*. IX. Characterization of insertion sequence-mediated mutations and rearrangements. Genetics **156:**477–488.
62. **Shaver, A. C., P. G. Dombrowski, J. Y. Sweeney, T. Treis, R. M. Zappala, and P. D. Sniegowski.** 2002. Fitness evolution and the rise of mutator alleles in experimental *Escherichia coli* populations. Genetics **162:**557–566.
63. **Simons, R. W., F. Houman, and N. Kleckner.** 1987. Improved single and

multicopy lac-based cloning vectors for protein and operon fusions. Gene **53:**85–96.
64. **Sniegowski, P. D., P. J. Gerrish, and R. E. Lenski.** 1997. Evolution of high mutation rates in experimental populations of *Escherichia coli*. Nature **387:** 703–705.
65. **Spratt, B. G.** 1975. Distinct penicillin binding proteins involved in the division, elongation, and shape of *Escherichia coli* K12. Proc. Natl. Acad. Sci. USA **72:**2999–3003.
66. **Spratt, B. G.** 1977. The mechanism of action of mecillinam. J. Antimicrob. Chemother. **3**(Suppl. B)**:**13–19.
67. **Spratt, B. G.** 1977. Properties of the penicillin-binding proteins of *Escherichia coli* K12. Eur. J. Biochem. **72:**341–352.
68. **Spratt, B. G., and A. B. Pardee.** 1975. Penicillin-binding proteins and cell shape in *E. coli*. Nature **254:**516–517.
69. **Takase, I., F. Ishino, M. Wachi, H. Kamata, M. Doi, S. Asoh, H. Matsuzawa, T. Ohta, and M. Matsuhashi.** 1987. Genes encoding two lipoproteins in the *leuS-dacA* region of the *Escherichia coli* chromosome. J. Bacteriol. **169:**5692–5699.
70. **Travisano, M., and R. E. Lenski.** 1996. Long-term experimental evolution in *Escherichia coli*. IV. Targets of selection and the specificity of adaptation. Genetics **143:**15–26.
71. **Tuomanen, E., and R. Cozens.** 1987. Changes in peptidoglycan composition and penicillin-binding proteins in slowly growing *Escherichia coli*. J. Bacteriol. **169:**5308–5310.
72. **Uehara, T., and J. T. Park.** 2002. Role of the murein precursor UDP-*N*-acetylmuramyl-L-Ala-γ-D-Glu-*meso*-diaminopimelic acid-D-Ala-D-Ala in repression of β-lactamase induction in cell division mutants. J. Bacteriol. **184:**4233–4239.
73. **van den Ent, F., M. Leaver, F. Bendezu, J. Errington, P. de Boer, and J. Löwe.** 2006. Dimeric structure of the cell shape protein MreC and its functional implications. Mol. Microbiol. **62:**1631–1642.
74. **Vasi, F., M. Travisano, and R. E. Lenski.** 1994. Long-term experimental evolution in *Escherichia coli*. II. Changes in life-history traits during adaptation to a seasonal environment. Am. Nat. **144:**432–456.
75. **Vinella, D., D. Joseleau-Petit, D. Thevenet, P. Bouloc, and R. D'Ari.** 1993. Penicillin-binding protein 2 inactivation in *Escherichia coli* results in cell division inhibition, which is relieved by FtsZ overexpression. J. Bacteriol. **175:**6704–6710.
76. **Vinella, D., R. D'Ari, A. Jaffe, and P. Bouloc.** 1992. Penicillin binding protein 2 is dispensable in *Escherichia coli* when ppGpp synthesis is induced. EMBO J. **11:**1493–1501.
77. **Vollmer, W., M. von Rechenberg, and J. V. Höltje.** 1999. Demonstration of molecular interactions between the murein polymerase PBP1B, the lytic transglycosylase MltA, and the scaffolding protein MipA of *Escherichia coli*. J. Biol. Chem. **274:**6726–6734.
78. **Weidel, W., and H. Pelzer.** 1964. Bagshaped macromolecules—a new outlook on bacterial cell walls. Adv. Enzymol. **26:**193–232.
79. **Woods, R., D. Schneider, C. L. Winkworth, M. A. Riley, and R. E. Lenski.** 2006. Tests of parallel molecular evolution in a long-term experiment with *Escherichia coli*. Proc. Natl. Acad. Sci. USA **103:**9107–9112.
80. **Yanisch-Perron, C., J. Vieira, and J. Messing.** 1985. Improved M13 phage cloning vectors and host strains: nucleotide sequences of the M13mp18 and pUC19 vectors. Gene **33:**103–119.
81. **Young, K. D.** 2001. Approaching the physiological functions of penicillin-binding proteins in *Escherichia coli*. Biochimie **83:**99–102.
82. **Young, K. D.** 2003. Bacterial shape. Mol. Microbiol. **49:**571–580.
83. **Yousif, S. Y., J. K. Broome-Smith, and B. G. Spratt.** 1985. Lysis of *Escherichia coli* by β-lactam antibiotics: deletion analysis of the role of penicillin binding proteins 1A and 1B. J. Gen. Microbiol. **131:**2839–2845.
84. **Zinser, E. R., and R. Kolter.** 1999. Mutations enhancing amino acid catabolism confer a growth advantage in stationary phase. J. Bacteriol. **181:**5800–5807.